HHS Public Access

Author manuscript

Sci Immunol. Author manuscript; available in PMC 2019 March 02.

Published in final edited form as:

Sci Immunol. 2018 March 02; 3(21): . doi:10.1126/sciimmunol.aao6923.

RORα-expressing T regulatory cells restrain allergic skin inflammation

Nidhi Malhotra[1,*,†,‡], **Juan Manuel Leyva-Castillo**[1,*,‡], **Unmesh Jadhav**[2,3], **Olga Barreiro**[4], **Christy Kam**[1], **Nicholas K. O'Neill**[2,3], **Francoise Meylan**[5], **Pierre Chambon**[6], **Ulrich H. von Andrian**[4], **Richard M. Siegel**[5], **Eddie C. Wang**[7], **Ramesh Shivdasani**[2,3], and **Raif S. Geha**[1,‡]

[1]Division of Immunology, Boston Children's Hospital, Harvard Medical School, Boston, MA 02115, USA

[2]Department of Medical Oncology and Center for Functional Cancer Epigenetics, Dana-Farber Cancer Institute, Boston, MA 02115, USA

[3]Department of Medicine, Harvard Medical School, Boston, MA 02115, USA

[4]Department of Microbiology and Immunobiology and Center for Immune Imaging, Harvard Medical School, Boston, MA 02115, USA

[5]Immunoregulation Section, Autoimmunity Branch, National Institute of Arthritis and Musculoskeletal and Skin Diseases, National Institutes of Health, Bethesda, MD 20892, USA

[6]Institut de Génétique et de Biologie Moléculaire et Cellulaire (CNRS UMR7104, INSERM U964), Illkirch 67404, France

[7]Department of Microbial Microbiology and Infectious Diseases, School of Medicine, Cardiff University, Cardiff, UK

Abstract

Atopic dermatitis is an allergic inflammatory skin disease characterized by the production of the type 2 cytokines in the skin by type 2 innate lymphoid cells (ILC2s) and T helper 2 (T_H2) cells, and tissue eosinophilia. Using two distinct mouse models of atopic dermatitis, we show that expression of retinoid-related orphan receptor α (RORα) in skin-resident T regulatory cells (T_{regs}) is important for restraining allergic skin inflammation. In both models, targeted deletion of RORα in mouse T_{regs} led to exaggerated eosinophilia driven by interleukin-5 (IL-5) production by ILC2s

[‡]Corresponding author. Email: nidhi.malhotra@elstartherapeutics.com (N.M.); manuel. leyvacastillo@childrens.harvard.edu (J.M.L.-C.); raif.geha@childrens.harvard.edu (R.S.G.).

[*]These authors contributed equally to this work.

[†]Present address: Elstar Therapeutics, 840 Memorial Drive, Cambridge, MA 02139, USA.

SUPPLEMENTARY MATERIALS

immunology.sciencemag.org/cgi/content/full/3/21/eaao6923/DC1

Author contributions: N.M., J.M.L.-C., and R.S.G. designed the experiments; N.M., J.M.L.-C., U.J., O.B., N.K.O., and C.K. performed the experiments and analyzed the data. F.M., P.C., U.H.v.A., R.M.S., E.C.W., and R.S. contributed critical reagents, mice, or analytic tools. N.M., J.M.L.-C., and R.S.G. interpreted the data and wrote the manuscript. N.M. and J.M.L.-C. performed the statistical analyses.

Competing interests: The authors declare that they have no competing interests.

Data and materials availability: The RNA-seq data reported in this paper are archived at the NCBI Gene Expression Omnibus database (accession no. GSE99086).

and T_H2 cells. Expression of RORα in skin-resident T_{regs} suppressed IL-4 expression and enhanced expression of death receptor 3 (DR3), which is the receptor for tumor necrosis factor (TNF) family cytokine, TNF ligand–related molecule 1 (TL1A), which promotes T_{reg} functions. DR3 is expressed on both ILC2s and skin-resident T_{regs}. Upon deletion of RORα in skin-resident T_{regs}, we found that T_{regs} were no longer able to sequester TL1A, resulting in enhanced ILC2 activation. We also documented higher expression of RORα in skin-resident T_{regs} than in peripheral blood circulating T_{regs} in humans, suggesting that RORα and the TL1A-DR3 circuit could be therapeutically targeted in atopic dermatitis.

INTRODUCTION

Atopic dermatitis (AD) is the most common skin inflammatory disease affecting ~17% of children in developed nations (1). AD lesions are characterized by the presence of activated T helper 2 (T_H2) cells, as well as by the expansion of type 2 innate lymphoid cells (ILC2s) (2–4). Both T_H2 cells and ILC2s may contribute to allergic skin inflammation in AD. Cutaneous inflammation elicited by topical application of calcipotriol (MC903), a low-calcemic analog of vitamin D, has been used as a mouse model of acute AD (5, 6). Allergic inflammation in this model is accompanied by expansion of ILC2s driven by epithelial cytokines (2, 4). More importantly, it is dependent on ILC2s; it is preserved in *Rag1*$^{-/-}$ mice and is severely attenuated in *Tslpr*$^{-/-}$ mice, ILC- depleted *Rag1*$^{-/-}$ mice, and ILC2-deficient *Rora*$^{sg/sg}$/wild-type (WT) bone marrow chimeras (2, 4). Cutaneous inflammation elicited by repeated epicutaneous (EC) application of ovalbumin (OVA) or peanut extract to tape-stripped mouse skin provides an antigen-driven mouse model of acute AD (7–9). Allergic inflammation in this model is dependent on T cells, because it is abolished in *Rag2*$^{-/-}$ mice (9, 10).

$CD4^+FOXP3^+$ T regulatory cells (T_{regs}) constitute a substantial subset of immune cells residing in murine and human skin (11). Lack of T_{regs} in humans and mice results in immune dysregulation associated with allergic skin inflammation (12, 13). T_{reg} numbers are unaltered in AD skin lesions (14). Thus, the role of skin-resident T_{regs} in controlling allergic skin inflammation is unclear. Here, we have dissected the molecular architecture of skin-resident T_{regs} and identified retinoid-related orphan receptor α (RORα) as a regulator of genes in T_{regs} responsible for suppressing allergic skin inflammation.

RESULTS

Skin-resident T_{regs} exhibit an activated signature and express the transcription factor RORα

Specialization of tissue-resident T_{regs} is an important factor in maintaining tissue homeostasis and modulating local immune responses. To investigate whether skin-resident T_{regs} exhibit a specialized phenotype, we compared the phenotype of skin-resident T_{regs} and T_{regs} in skin-draining lymph node (dLN). About 45% of $CD4^+$ T cells in ear skin expressed FOXP3 compared with ~20% of $CD4^+$ T cells in dLNs (Fig. 1A). Skin T_{regs} localized around dermal blood vessels and interfollicular areas (fig. S1A). We compared the transcriptome of $CD3^+CD4^+YFP^+$ T_{regs} from the skin and dLN of *Foxp3*$^{eyfp\text{-}cre}$ mice. Skin

T_{regs} differed from dLN T_{regs} by more than 5000 genes [fold change > 2; false discovery rate (FDR) < 0.05]. Skin T_{regs} were enriched for the expression of genes encoding signaling receptors [*Icos and Il1rl1* (ST2)], activation markers (*Cd44* and *Klrg1*), effector molecules (*Il10*, *Ctla4*, and *Areg*), and tissue-homing receptors (*Ccr3, Ccr8*, and *Ccr10*) (Fig. 1B). Flow cytometry demonstrated that the percentage of T cells that expressed ST2, ICOS, and CD44 and the expression levels of these markers were significantly higher in skin T_{regs} than in dLN T_{regs} (Fig. 1C). *Rora*, the gene encoding the transcriptional regulator RORα, was highly up-regulated in skin T_{regs} (Fig. 1B). This was confirmed by quantitative polymerase chain reaction (qPCR) (Fig. 1D). *RORA* expression was significantly higher in $CD4^+CD25^+CD127^{lo}$ skin T_{regs} than in circulating T_{regs} in humans (Fig. 1E). Human skin T_{regs}, similar to mouse skin T_{regs}, display an activated signature with increased expression of ICOS, CTLA4, and CD44 (15).

To examine and map the fate of RORα-expressing T_{regs}, we bred $Rora^{cre}$ mice to *Rosa26Yfp* (R26Y) mice. In $Rora^{cre}$R26Y mice, yellow fluorescent protein (YFP) marks cells that are expressing or previously expressed *Rora*. Most of the skin T_{regs} (>90%) in $Rora^{cre}$R26Y mice expressed YFP compared with a small fraction (~5%) of T_{regs} from dLNs (Fig. 1F). $Rora^+$(YFP^+) T_{regs} in the skin uniformly expressed the transcription factor HELIOS, but not RORγt (fig. S1B), suggesting that RORα-expressing skin T_{regs} are natural T_{regs}. The percentage of $ICOS^+$ and $ST2^+$ T_{regs} and the levels of ICOS and ST2 were significantly higher in $Rora^+$(YFP^+) T_{regs} than in $Rora^-$(YFP^-) T_{regs} in dLNs (fig. S1C). A negligible subset (<1%) of thymic T_{regs} were $Rora^+$(YFP^+) (fig. S1D), suggesting that $ROR\alpha^+$ T_{regs} expand and/or are induced in peripheral tissues.

We used $Rora^{cre}$R26Y mice to investigate *Rora* expression by cell subpopulations in the skin. In addition to T_{regs}, a fraction of $CD3^+CD4^+CD25^-$ T cells, $CD3^+CD8^+$ T cells, $CD3^+TCR\gamma\delta^{+/low}$ dermal γδ T cells, $CD3^+TCR\gamma\delta^{high}$ epidermal γδ T cells, and $CD45^+Lin^-$ ILCs in the skin were YFP^+ ($Rora^+$) (fig. S2A). In addition, a fraction of $CD45^-EpCAM^+$ keratinocytes that are mostly derived from the basal layer of the epidermis and a fraction of $CD45^-EpCAM^-$ cells, which contain a mixture of mature keratinocytes and fibroblasts in the skin, were YFP^+ ($Rora^+$) (fig. S2A). The percentages of YFP^+ ($Rora^+$) cells among skin cell subpopulations were not significantly altered following MC903 treatment (fig. S2, B and C). These results show that RORα expression was not restricted to skin T_{regs}.

RORα deficiency in T_{regs} results in exaggerated allergic skin inflammation in response to topical application of MC903

RORα is necessary for the development of ILC2s (16), promotes T_H17 cell differentiation, and antagonizes FOXP3 in vitro (17), suggesting a potential pro-inflammatory role. To understand how RORα regulates the function and/or maintenance of skin T_{regs}, we generated $Foxp3^{eyfp\text{-}cre}Rora^{fl/fl}$ mice. Fluorescence-activated cell sorting (FACS) analysis of skin population of cells from $Foxp3^{egfp}$ mice for enhanced green fluorescent protein (eGFP) expression revealed that *Foxp3* expression was restricted to $CD4^+$ T cells and was not detected in any other additional skin cell population that expressed *Rora* in the skin, including $CD8^+$ T cells, dermal and epidermal γδ T cells, ILCs, and $CD45^-$ cells (fig. S3). In addition, none of the $Foxp3^{eyfp\text{-}cre}Rora^{fl/fl}$ mice had weight loss or developed the

staggerer phenotype observed in RORα-deficient *Rora*$^{sg/sg}$ mice (18). Furthermore, the numbers of ILCs and γδ T cells in the skin were not reduced in *Foxp3*$^{eyfp\text{-}cre}$*Rora*$^{fl/fl}$ mice. These results suggest that *Rora* is deleted specifically in T_{regs} of *Foxp3*$^{eyfp\text{-}cr}$ *Rora*$^{fl/fl}$ mice. RNA sequencing (RNA-seq) analysis of T_{regs} revealed complete deletion of the floxed fourth exon of *Rora* in these mice (fig. S4A). The numbers of YFP$^+$ T_{regs} were not altered in the skin or dLNs of these mice (fig. S4B), indicating that RORα is not required for the accumulation or maintenance of T_{regs} in the skin. The cytokine interleukin-10 (IL-10) is important for T_{reg} function in the gut and lungs (19). There was an increased percentage of IL-10$^+$ T_{regs} in *Foxp3*$^{eyfp\text{-}cre}$*Rora*$^{fl/fl}$ mice compared with controls (fig. S4C).

Topical application of MC903 to ear skin of WT mice results in increased dermal thickness and infiltration of CD45$^+$ cells that include eosinophils and CD4$^+$ T cells (5). There was an increased ear thickness, accompanied with an intense cellular infiltrate, and significantly increased dermal thickness in *Foxp3*$^{eyfp\text{-}cre}$*Rora*$^{fl/fl}$ mice compared with *Foxp3*$^{eyfp\text{-}cre}$ controls (Fig. 2, A to C). FACS analysis revealed a threefold increase in dermal infiltration by CD45$^+$ cells in *Foxp3*$^{eyfp\text{-}cre}$*Rora*$^{fl/fl}$ mice compared with *Foxp3*$^{eyfp\text{-}cre}$ controls (Fig. 2D). Eosinophils accounted for ~45% of CD45$^+$ cells in the dermis of MC903-treated *Foxp3*$^{eyfp\text{-}cre}$*Rora*$^{fl/fl}$ mice, compared with 15% in controls, yielding an eightfold increase in eosinophil numbers (Fig. 2E). The percentages of basophils (ckit$^-$IgE$^+$), mast cells (ckit$^+$IgE$^+$), neutrophils (CD11b$^+$Gr1^{hi}), T effector cells (T_{effs}) (CD4$^+$FOXP3$^-$), T_{regs} (CD4$^+$FOXP3$^+$), and ILCs (Lin$^-$CD90$^+$) infiltrating MC903-treated skin were comparable in *Foxp3*$^{eyfp\text{-}cre}$*Rora*$^{fl/fl}$ mice and controls. Nevertheless, the numbers of these cell populations were two- to threefold higher in *Foxp3*$^{eyfp\text{-}cre}$*Rora*$^{fl/fl}$ mice (Fig. 2, F and G), reflecting the approximately threefold increase in CD45$^+$ cells. MC903-driven allergic inflammation in mice of C56BL/6 background is largely dependent on thymic stromal lymphopoietin (TSLP) (2, 4). The exaggerated cutaneous inflammatory response in *Foxp3*$^{eyfp\text{-}cre}$*Rora*$^{fl/fl}$ mice, which are on a C56BL/6 background, was not due to increased *Tslp* expression (fig. S5A). Serum immunoglobulin E (IgE) levels were higher in MC903-treated *Foxp3*$^{eyfp\text{-}cre}$*Rora*$^{fl/fl}$ mice than in controls (fig. S5B), indicative of a heightened type 2 response.

RORα deficiency in T_{regs} results in increased expression of eotaxins and IL-5 in MC903-treated skin

The proportion of eosinophils in blood was comparable in MC903-treated *Foxp3*$^{eyfp\text{-}cre}$*Rora*$^{fl/fl}$ mice and controls (fig. S6A), suggesting that the exaggerated eosinophilia in MC903-treated skin of *Foxp3*$^{eyfp\text{-}cre}$*Rora*$^{fl/fl}$ mice resulted from increased eosinophil recruitment. Eotaxins are the major eosinophil chemoattractants (20). There was increased expression of *Ccl11* and *Ccl24*, which encode for eotaxins 1 and 2, in MC903-treated skin of *Foxp3*$^{eyfp\text{-}cre}$*Rora*$^{fl/fl}$ mice compared with controls (Fig. 3A). IL-5 plays a critical role in tissue eosinophilia by synergizing with eotaxins and promoting eosinophil survival in tissues (21, 22). IL-5 levels were significantly higher in MC903-treated skin of *Foxp3*$^{eyfp\text{-}cre}$*Rora*$^{fl/fl}$ mice than of controls (Fig. 3B). IL-4 and IL-13 levels were comparable in the two groups (fig. S6B).

IL-5 is predominantly produced by ILC2s and by a subset of activated T_H2 cells (23). ILC2s exist as preactivated resident sentinels in the dermis that rapidly release IL-5 and IL-13 upon

stimulation (21). In contrast, T_H2 cells are recruited to the skin at a later stage of allergic inflammation. MC903 treatment up-regulated IL-33/ST2 and CD69 expression, down-regulated CD25 expression, and had negligible effect on KLRG1 expression on skin Lin $^-$CD90$^+$ ILCs, but the changes were comparable in *Foxp3*$^{eyfp\text{-}cre}$*Rora*$^{fl/fl}$ mice and *Foxp3*$^{eyfp\text{-}cre}$ controls. However, in *Il5*, mRNA levels were significantly increased in ILCs from MC903-treated skin of *Foxp3*$^{eyfp\text{-}cre}$*Rora*$^{fl/fl}$ mice compared with controls (Fig. 3C). There was also a twofold increase in *Il4* and *Il13* mRNA levels in ILCs from MC903-treated skin of *Foxp3*$^{eyfp\text{-}cre}$*Rora*$^{fl/fl}$ mice; however, it did not reach statistical significance (fig. S6C). There was a significant increase in CD4$^+$FOXP3$^-$IL-5$^+$, but not CD4$^+$IL-13$^+$ or CD4$^+$IL-4$^+$, T_{effs} in *Foxp3*$^{eyfp\text{-}cre}$*Rora*$^{fl/fl}$ mice compared with controls (Fig. 3D). The chemokine CCL8 is up-regulated in AD skin lesions (24) and is critical for the recruitment of CCR8-expressing IL-5$^+$ T_H2 cells to the skin in a mouse model of AD (24). *Ccl8* expression was strongly increased in MC903-treated skin of *Foxp3*$^{eyfp\text{-}cre}$*Rora*$^{fl/fl}$ mice (Fig. 3E). In contrast, *Ccl17*, *Ccl22*, *Ccl4*, and *Ccl5* expression was comparable in *Foxp3*$^{eyfp\text{-}cre}$*Rora*$^{fl/fl}$ mice and controls (fig. S6D). *Cxcl1*, *Ccl2*, and *Ccl7* expression demonstrated a trend toward an increase in MC903-treated skin of *Foxp3*$^{eyfp\text{-}cre}$*Rora*$^{fl/fl}$ mice, which could underlie the increased influx of myeloid cells in these mice (Fig. 2F).

RORα deficiency in T_{regs} alters the expression of genes involved in T_{reg} cell migration and function and skews T_{regs} to IL-4–producing effectors

To gain an understanding of how RORα regulates the function of skin T_{regs}, we performed next-generation sequencing (NGS) transcriptomic analysis on T_{regs} isolated from untreated and MC903-treated skin of *Foxp3*$^{eyfp\text{-}cre}$*Rora*$^{fl/fl}$ mice and *Foxp3*$^{eyfp\text{-}cre}$ controls (table S1 and fig. S7). We observed a change in ~1700 genes across the four groups examined (fold change > 2; FDR < 0.05) (Fig. 4A). Expression of the central circadian rhythm genes *Nr1d1* and *Nr1d2* was decreased in skin T_{regs} from *Foxp3*$^{eyfp\text{-}cre}$*Rora*$^{fl/fl}$ mice compared with controls, consistent with the role of RORα as a circadian rhythm regulator (25). Genes involved in signaling via transforming growth factor–β (TGFβ) (*Smad3*), tumor necrosis factor–α (TNFα) (*Tnfa*), nuclear factor κB (NF-κB) (*Irak4* and *Tirap*), and mitogen-activated protein kinase (MAPK) (*Fos* and *Jun*) and in cell adhesion (*Icam2* and *Itga4)* were comparably expressed in T_{regs} from untreated skin of *Foxp3*$^{eyfp\text{-}cre}$*Rora*$^{fl/fl}$ mice and *Foxp3*$^{eyfp\text{-}cre}$ controls and underwent comparable changes after MC903 treatment. Genes in the phosphatidylinositol 3-kinase (PI3K)/AKT pathway were down-regulated in RORα-deficient skin T_{regs}. Dysregulated PI3K/AKT signaling affects *Foxp3* and *Il2ra* expression in T_{regs} and increases their conversion to T_H1 cells (26). We did not observe any effect on *Foxp3*, *Il2ra*, or *Ifng* expression in our transcriptomic and flow cytometric analyses of skin T_{regs} from *Foxp3*$^{eyfp\text{-}cre}$*Rora*$^{fl/fl}$ mice. Several genes encoding chemokines and chemokine receptors (*Ccl2*, *Ccr3*, and *Ccr5*) were up-regulated upon allergic skin inflammation in all mice, but to greater extent in *Foxp3*$^{eyfp\text{-}cre}$*Rora*$^{fl/fl}$ mice. Up-regulation of these genes is consistent with the increased numbers, and higher velocity, of T_{regs} in MC903-treated skin of *Foxp3*^{egfp} mice (Fig. 2G; fig. S8, A and B; and movies S1 and S2). Furthermore, T_{regs} in MC903- treated skin showed less directed movement (fig. S8C). Expression of *Ccr6* and CCR6, thought to be important for migration of T_{regs} into neonatal skin (27), was strongly decreased in skin T_{regs} from *Foxp3*$^{eyfp\text{-}cre}$*Rora*$^{fl/fl}$ mice compared with controls both before

and after MC903 treatment (Fig. 4, A to C). However, the numbers of skin T_{regs} in *Foxp3*$^{eyfp\text{-}cre}$*Rora*$^{fl/fl}$ mice were not reduced (Fig. 3G).

T_{reg} suppressive activity is mediated in part by the nucleotides adenosine and cyclic adenosine 3′,5′-monophosphate (cAMP) (28). T_{regs} from untreated and MC903-treated skin showed strongly decreased expression of *Nt5e*, which encodes the 5′ ectonucleotidase CD73 that metabolizes AMP to adenosine (28), and reduced surface expression of CD73 compared with controls (Fig. 4, B and D), whereas expression of *Pde3b*, which encodes the phosphodiesterase 3B that breaks down cAMP (29), was increased (Fig. 4B). Expression of *Gzmb*, which encodes granzyme B that mediates T_{reg} cytotoxic activity, was up-regulated (Fig. 4B), indicating that not all genes involved in T_{reg} function were down-regulated in the absence of RORα.

Expression of IL-4 in T_{regs} inhibits their ability to suppress T_H2 cells and ILC2s (30, 31). *Il4* levels were elevated in skin T_{regs} from *Foxp3*$^{eyfp\text{-}cre}$*Rora*$^{fl/fl}$ mice compared with controls (Fig. 4, A and B). This was confirmed by qPCR (Fig. 4E). Furthermore, the percentage of $CD4^+Foxp3^+$ T_{regs} among IL-4–expressing $CD4^+$ cells in MC903- treated skin was significantly higher in *Foxp3*$^{eyfp\text{-}cre}$*Rora*$^{fl/fl}$ mice than in controls (Fig. 4F). These results suggest that RORα expression prevents the conversion of T_{regs} into IL-4–producing effectors. The transcription factor RUNX1 inhibits *Il4* expression in T_{regs} (32). *Runx1* expression was decreased in T_{regs} from *Foxp3*$^{eyfp\text{-}cre}$*Rora*$^{fl/fl}$ mice (Fig. 5B), suggesting that reduced RUNX1 activity may derepress *Il4* expression in RORα- deficient T_{regs}. T_{regs} from MC903-treated skin of *Foxp3*$^{eyfp\text{-}cre}$*Rora*$^{fl/fl}$ mice, but not controls, expressed *Ccl8* and *Ccl24* transcripts (Fig. 4B), suggesting that these T_{regs} contribute to the exaggerated eosinophil-dominated allergic skin inflammation in *Foxp3*$^{eyfp\text{-}cre}$*Rora*$^{fl/fl}$ mice.

RORα expression in T_{regs} promotes expression of the TL1A ligand DR3 and restrains TL1A-driven allergic inflammation elicited by cutaneous application of MC903

Tnfrsf25 encodes the TNF receptor family member DR3 (death receptor 3), which is expressed constitutively on T cells, including T_{regs} and ILC2s (33, 34). *Tnfrsf25* expression, as determined by RNA-seq analysis, and DR3 surface expression, as determined by FACS analysis, were both strongly reduced in skin T_{regs} from *Foxp3*$^{eyfp\text{-}cre}$*Rora*$^{fl/fl}$ mice compared with *Foxp3*$^{eyfp\text{-}cre}$ controls (Figs. 4B and 5, A and B). In contrast, DR3 surface expression by skin ILC2s was comparable in *Foxp3*$^{eyfp\text{-}cre}$*Rora*$^{fl/fl}$ mice and controls (Fig. 5C). The DR3 ligand TL1A is released by endothelial and myeloid cells. TL1A synergizes with the epithelial cytokines IL-33, IL-7, and IL-25 to enhance IL-5 expression in human and murine ILC2s and to promote allergic inflammation (33, 35, 36). TL1A also acts on T_{regs} to increase their proliferation and their ability to suppress allergic airway inflammation (34). Skin TL1A levels were not altered after MC903 treatment and were comparable in *Foxp3*$^{eyfp\text{-}cre}$*Rora*$^{fl/fl}$ mice and *Foxp3*$^{eyfp\text{-}cre}$ controls (Fig. 5D). Given this finding, we tested the hypothesis that selective down-regulation of the TL1A receptor DR3 on T_{regs} from skin of *Foxp3*$^{eyfp\text{-}cre}$*Rora*$^{fl/fl}$ mice may play an important role in the exaggerated MC903-driven allergic inflammation observed in these mice. MC903-mediated eosinophilia was attenuated in *Tnfrsf25*$^{-/-}$ mice (Fig. 5E), demonstrating a role for TL1A in MC903-driven allergic skin inflammation. Intradermal injection of TL1A into ear skin resulted in a significant increase

in the percentage and numbers of eosinophils, but not neutrophils, in *Foxp3*$^{eyfp\text{-}cre}$*Rora*$^{fl/fl}$ mice compared with controls (Fig. 6F). More importantly, local TL1A blockade during MC903 treatment by intradermal injection of neutralizing antibody to TL1A significantly reduced MC903-driven allergic skin inflammation in *Foxp3*$^{eyfp\text{-}cre}$*Rora*$^{fl/fl}$ mice. This was evidenced by a significant decrease in dermal thickness, infiltration by CD45$^+$ cells and eosinophils, and expression of *Il5* and *Ccl8* compared with isotype control antibody–treated mice (Fig. 6, G to J). These results suggest that RORα expression in T_{regs} restrains TL1A-mediated allergic skin inflammation and eosinophilia elicited by cutaneous application of MC903.

RORα deficiency in T_{regs} results in exaggerated skin inflammation in response to EC sensitization

To investigate whether RORα deficiency in T_{regs} plays a role in restraining antigen-driven T cell–dependent allergic skin inflammation, we subjected *Foxp3*$^{eyfp\text{-}cre}$*Rora*$^{fl/fl}$ mice and *Foxp3*$^{eyfp\text{-}cre}$ controls to EC sensitization. EC sensitization was elicited by repeated application of the antigen OVA to tape-stripped skin, as illustrated in Fig. 6A. Skin inflammation in this model shares many characteristics of acute AD skin lesions, including epidermal thickening, dermal infiltration by CD45$^+$ cells (including eosinophils), and increased expression of type 2 cytokines (8, 9). *Foxp3*$^{eyfp\text{-}cre}$*Rora*$^{fl/fl}$ mice EC sensitized with OVA exhibited significantly increased epidermal thickness and significantly increased infiltration by CD45$^+$ cells compared with *Foxp3*$^{eyfp\text{-}cre}$ controls EC sensitized with OVA (Fig. 6, B to D). Furthermore, the numbers of all cell populations analyzed, including eosinophils, basophils, neutrophils, mast cells, CD4$^+$Foxp3$^-$ T cells, T_{regs}, and ILCs, were two-to fourfold higher in OVA-sensitized skin of *Foxp3*$^{eyfp\text{-}cre}$*Rora*$^{fl/fl}$ mice compared with *Foxp3*$^{eyfp\text{-}cre}$ controls (Fig. 6, E and F). *Il4*, but not *Il13*, mRNA levels in OVA-sensitized skin were significantly higher in *Foxp3*$^{eyfp\text{-}cre}$*Rora*$^{fl/fl}$ mice than in controls (Fig. 6G). *Il5* mRNA was not detectable in sensitized skin in either group. Nevertheless, intracellular FACS analysis revealed that OVA sensitization caused a small but significant increase in the numbers of IL-5$^+$ ILCs and IL-5$^+$ CD4$^+$FOXP3$^-$ T_{effs} in *Foxp3*$^{eyfp\text{-}cre}$ control mice. The numbers of IL-5$^+$ ILCs and IL-5$^+$ CD4$^+$FOXP3$^-$ T_{effs} were four- to fivefold higher in OVA-sensitized skin of *Foxp3*$^{eyfp\text{-}cre}$*Rora*$^{fl/fl}$ mice than in controls (Fig. 6H). OVA sensitization did not result in significant changes in IL-33R/ST2, CD69, CD25, or KLRG1 expression by skin ILCs in *Foxp3*$^{eyfp\text{-}cre}$*Rora*$^{fl/fl}$ or *Foxp3*$^{eyfp\text{-}cre}$ controls. These results suggest that RORα$^+$ T_{regs} play an important role in constraining antigen-driven skin inflammation.

DISCUSSION

We show that skin T_{regs} express high levels of the transcription factor RORα. Deletion of *Rora* in T_{regs} does not alter the number of skin T_{regs} but results in exaggerated type 2 allergic skin inflammation in response to topical application of MC903 or EC sensitization with OVA. Thus, we have identified RORα as a regulator of T_{reg} genes responsible for suppressing allergic skin inflammation.

The vast majority of mouse skin T_{regs} expressed RORα and had an activated phenotype. In contrast, a small minority of T_{regs} in skin dLNs expressed RORα and had an activated

phenotype. It remains to be determined whether circulating RORα$^+$ T_{regs} are specifically attracted to the skin or whether the skin environment drives RORα expression in T_{regs}. The numbers of skin T_{regs} are not altered in *Foxp3*$^{eyfp\text{-}cre}$*Rora*$^{fl/fl}$ mice. Furthermore, although the majority of human blood T_{regs} express the skin-homing receptor CLA (37), human blood T_{regs} expressed fivefold less *RORA* mRNA compared with skin T_{regs}. These findings argue for local acquisition of RORα expression by T_{regs} in the skin.

We demonstrated that RORα expression in T_{regs} restrains allergic skin inflammation induced by topical application of MC903, an AD model dependent on ILC2s (2, 4). This was evidenced by increased ear swelling and dermal thickness in *Foxp3*$^{eyfp\text{-}cre}$*Rora*$^{fl/fl}$ mice, with a threefold increase in the influx of inflammatory cells that included T cells, basophils, neutrophils, and mast cells, and a selective enrichment in eosinophils that showed an eightfold increase over controls. Type 2 cytokines, such as IL-4, are documented to drive eotaxin expression (21, 38). Increased eosinophilia in MC903-treated skin of *Foxp3*$^{eyfp\text{-}cre}$*Rora*$^{fl/fl}$ mice may be explained by synergy between increased skin IL-5 expression and increased skin and T_{regs} eotaxin expression, likely driven by increased expression of IL-4 and IL-13. The exaggerated skin inflammation in *Foxp3*$^{eyfp\text{-}cre}$*Rora*$^{fl/fl}$ mice was not caused by increased cutaneous expression of TSLP, the epithelial cytokine essential for MC903-driven skin inflammation in mice on the C57BL/6 background, the background of the *Foxp3*$^{eyfp\text{-}cre}$*Rora*$^{fl/fl}$ mice we used. RORα was essential for repressing IL-5 expression in fast- responding ILC2s and for restricting the CCL8-dependent recruitment of IL-5$^+$ T_H2 effector cells to the skin, likely by dampening the expression of *Ccl8* in the skin, and particularly in skin T_{regs}. RORα also repressed IL-13 and IL-4 expression by skin ILCs, although the effect did not reach statistical significance, but had no effect on IL-4 and IL-13 expression by T cells. We propose that in addition to their role in restraining adaptive immunity, a central function of T_{regs} resident in barrier interfaces, such as skin, is to inhibit the rapid activation of innate lymphocytes. The unrestrained activation of these innate sentinels may contribute to acute flare-ups in allergic diseases.

RORα regulated the expression of several genes important for T_{reg} migration and function. Changes in chemokine receptor expression may underlie the increased motility of T_{regs} in *Foxp3*$^{eyfp\text{-}cre}$*Rora*$^{fl/fl}$ mice. Our data suggest that decreased expression by RORα-deficient T_{regs} of *Tnfrsf25* encoding DR3, a gene important for T_{reg} function, contributed to the enhanced skin inflammation in *Foxp3*$^{eyfp\text{-}cre}$*Rora*$^{fl/fl}$ mice. The exaggerated skin inflammation in *Foxp3*$^{eyfp\text{-}cre}$*Rora*$^{fl/fl}$ mice may be a direct effect of decreased TL1A activation of T_{regs} and/or increased availability of TL1A to activate ILC2s. Definitive evidence of the role of DR3 expression on T_{regs} in limiting allergic skin inflammation and its mechanism of action awaits the generation and study of mice with selective deficiency of *Tnfrsf25* in T_{regs} and/or ILC2s. Furthermore, our data indicate that RORα restrains the conversion of T_{regs} into IL-4–producing effector cells, possibly because RORα drives the expression of *Runx1*, which inhibits *Il4* gene transcription. Derepression of the T_H2 proinflammatory genes in RORα-deficient skin T_{regs} likely contributes to the enhanced allergic skin response in *Foxp3*$^{eyfp\text{-}cre}$*Rora*$^{fl/fl}$ mice. Furthermore, IL-10 expression was increased in RORα-deficient skin T_{regs}. The transcription factor AhR (aryl hydrocarbon receptor) enhances IL-10 production in T_{regs} (39), whereas IL-4 suppresses it (40). We

observed increased *Ahr* and *Il4* expression in RORα-deficient skin T_{regs}. Increased expression of AhR and IL-4 may underlie the enhanced IL-10 expression by these cells.

In addition to its role in suppressing ILC2-dependent allergic skin inflammation driven by topical application of MC903, RORα expression in T_{regs} was important for suppressing T cell–dependent allergic skin inflammation driven by topical application of the antigen OVA to tape-stripped skin, a T cell–dependent mouse model of AD. This was evidenced by increased epidermal thickness, increased dermal infiltration by $CD45^+$ inflammatory cells (including eosinophils, mast cells, neutrophils, T cells, and ILC2s), increased cutaneous expression of *Il4*, and increased expression of IL-5 by T cells and ILCs.

We demonstrate significantly higher expression of *RORA* in human skin T_{regs} than in blood T_{regs}, suggesting that our results may be applicable to humans. Our results may be particularly relevant to patients with AD, a disease in which both T_H2 cells and ILC2s play important roles in allergic skin inflammation. *RORA* polymorphisms in asthma (41) and *Rora* down-regulation in dogs with AD (42) further suggest that RORα may play a regulatory role in atopic diseases. Moreover, expression of *Rora* in T_{regs} resident in tissues such as the gut (43) may endow them with the ability to dampen allergic inflammation in organs other than skin.

MATERIALS AND METHODS

Mice

Foxp3$^{eyfp\text{-}cre}$ (C57BL/6), R26R (C57BL/6), *Rag1*$^{-/-}$ (C57BL/6), and *Rorc*^{gfp} (C57BL/6) mice were purchased from the Jackson Laboratory (Bar Harbor, ME). *Rora*$^{fl/fl}$ (C57BL/6) mice were generated in the laboratory of P. Chambon (France) (44). *Rora*^{cre} (C57BL/6) mice were generated in the laboratory of D. O'Leary (45). *Tnfrsf25*$^{-/-}$ mice were generated by E. Y. Wang and obtained from the laboratory of R. Siegel. *Foxp3*^{egfp} reporter mice were a gift from T. Chatila. All mice were kept in a pathogen-free environment. All procedures performed on the mice were in accordance with the Animal Care and Use Committee of the Children's Hospital Boston.

Preparation of skin cell homogenates from mice and human skin

Dorsal and ventral ear murine skin was separated using tweezers, chopped, and digested in complete Dulbecco's modified Eagle's medium containing Liberase TL (2.5 mg/ml, Roche, Life Technologies) and deoxyribonuclease (DNase) I (20 ng/ml, Sigma) for 90 min at 37°C, with vigorous shaking. Digested tissue was mechanically disrupted with a plunger, filtered, washed, and suspended in media for flow cytometric analysis. Human skin surgical discards of facial skin were obtained from the laboratory of R. Clark (Brigham and Women's Hospital). To obtain cells from human skin, we removed all the fat using a scalpel and chopped the skin into small pieces and digested for 2 hours at 37°C with vigorous shaking in complete RPMI containing collagenase IV (2 ng/ml, Worthington Pharmaceuticals), hyaluronidase (2 ng/ml, Sigma), and DNase I. Digested tissue was mechanically disrupted using a plunger, filtered, centrifuged, and resuspended for cell sorting.

Flow cytometry

All antibodies were obtained from eBioscience and BioLegend, except anti-mouse Siglec-F, which was purchased from BD Biosciences. Cells were preincubated with Fcγ receptor–specific blocking monoclonal antibody (2.4G2) and washed before staining. Staining with CD45 and fixable viability dye (eBioscience) was used for FACS analysis of skin cell homogenates. One hundred twenty-three count beads from eBioscience were used for estimating cell counts. Cells were analyzed on LSRFortessa (BD Biosciences), and the data were analyzed with FlowJo software (v9.7).

Intracellular staining analysis for cytokines and transcription factors

LN and skin cell suspensions were incubated with media containing phorbol 12,13-dibutyrate, ionomycin, GolgiPlug, and GolgiStop for 3 hours. Staining for surface markers was performed, followed by fixation and permeabilization using BD Cytofix/Cytoperm buffer. Cells were incubated with antibodies against cytokines, IL-4, IL-5, and IL-13, along with antibodies to FOXP3, overnight in Perm/Wash buffer (BD Biosciences). This protocol was also used to stain cells with anti-FOXP3 and anti-HELIOS markers without quenching the emission of YFP in *Rora*^{cre} R26R mice.

MC903 treatment

MC903 (catalog no. 2700) was purchased from Tocris Biochemicals. The stock was reconstituted in ethanol. MC903 (2 nM) (in a volume of 20 ml) was topically applied on the ears of mice every other day, for a total of four applications. Ethanol (vehicle) was applied on the control ear. Mice were sacrificed 1 day after the last application.

RNA preparation and qPCR

Cells were sorted directly into the lysis buffer of RNA Isolation Micro kit (Zymo Research), and RNA was prepared on the basis of kit instructions. For analysis of transcripts in skin, skin tissue was stored in RNAlater (Ambion) and homogenized using a tissue homogenizer, and RNA was prepared using RNA isolation kits (Zymo Research). Reverse transcription was performed with an iScript cDNA synthesis kit (Bio-Rad Laboratories). PCRs were run on an ABI Prism 7300 (Applied Biosystems) sequence detection system platform. TaqMan primers and probes were obtained from Life Technologies. The housekeeping gene *β$_2$-microglobulin* was used as a control. Relative mRNA expression was quantified using the $2^{-\Delta\Delta Ct}$ method.

RNA-seq and transcriptomic analysis

$CD3^+CD4^+Foxp3^+(YFP^+)$ T_{regs} from skin and dLNs were sorted on Aria cell sorter into the lysis buffer (PicoPure RNA Isolation kit, Life Technologies). RNA was prepared after DNase treatment (Qiagen) and sent to Dana-Farber Cancer Institute Molecular Biology Core Facility for library preparation and sequencing. Replicates with a minimum RIN (RNA integrity number) score of 7 were processed. Complementary DNA (cDNA) was synthesized using Clontech SMART-Seq v4 reagents from 500 pg of RNA and fragmented to a mean size of 150 base pairs (bp) with a Covaris M220 ultrasonicator. Illumina libraries were prepared from cDNA using Rubicon Genomics ThruPLEX DNA-seq reagents according to

the manufacturer's protocol. The finished double- stranded DNA libraries were quantified and sequenced on a single Illumina NextSeq 500 sequencing system run with single-end 75-bp reads by the Dana-Farber Cancer Institute Molecular Biology Core Facility. TopHat was used to align reads to mouse genome [Mm9, National Center for Biotechnology Information (NCBI)], and HTSeq was used to estimate read counts. Read counts from all experiments are listed in table S1. Highly correlated triplicate samples were used for comparative analysis (fig. S6). DEseq2 was used to normalize data and access differential gene expression with an FDR of <0.05. Expression levels for individual genes are represented as reads per kilobase of transcript per million mapped reads (RPKM). Heat maps were generated using GENE-E software (Broad Institute). RNA-seq raw data can be accessed through accession no. GSE99086.

Intravital two-photon imaging

Foxp3^{egfp} (Balb/c) mice were anesthetized intraperitoneally using ketamine (100 mg/kg) and xylazine (10 mg/kg). One of the ears was gently attached to an aluminum block using double-sided tape. Ear temperature was maintained at 33°C using a heating pad. GenTeal (Novartis) eye gel was spread over the ear to allow immersion of the 20× objective (0.95 numerical aperture). Images were acquired using an upright microscope (Prairie Technologies) coupled to a Mai Tai Ti:Sapphire laser (Spectra-Physics). To visualize vasculature, mice were intravenously injected with Qdot655 (Molecular Probes) diluted in phosphate-buffered saline. Images were acquired with a laser wavelength of 900 nm for optimal GFP excitation and second- harmonic generation. Epidermis and dermis were analyzed by acquisition of ~100-mm optical stacks every 30 to 60 s for 15 to 60 min with 4-mm spacing. Images were transformed into four-dimensional time-lapse movies and analyzed using Imaris software versions 7.4.2 and 8.4.1 (Bitplane). Imaging experiments were performed in the Balb/c background, but similar results were observed using *Foxp3*^{egfp} (C57BL/6) mice. Balb/c mice were preferred to avoid autofluorescence from melanin.

Histology

Tissue samples were stored in 10% formalin and sent to the histology core at Boston Children's Hospital for processing and hematoxylin and eosin (H&E) staining. Slides were analyzed on the 20× objective of bright-field microscope (Nikon), and captured images were analyzed using ImageJ software for enumeration of dermal thickness.

Local treatments by intradermal injection

Recombinant TL1A (0.9 μg/μl; catalog no. 753008, BioLegend) was injected intradermally into the ear of mice in a total volume of 10 ml every day for 3 days. Isotype antibody or anti-human/mouse TL1A antibody (R&D Systems) was injected intradermally into the ears in a total volume of 10 μl every other day for 3 days. Cells from ears were prepared, and flow cytometric analysis was performed as described earlier.

Epicutaneous sensitization

Six- to 8-week-old female mice were epicutaneously sensitized for 2 weeks, as described previously (9). In brief, for each treatment, female mice were anesthetized, and then their

back skin was shaved and tape-stripped with a film dressing (Tegaderm, 3M). EC sensitization consisted of applying a 1-cm^2 gauze containing 200 μg of OVA (Sigma-Aldrich) to the skin after each tape stripping and securing it with a film dressing. Analyses were done at day 12.

Enzyme-linked immunosorbent assays

For detection of total IgE levels, mouse sera were prepared and enzyme- linked immunosorbent assay (ELISA) was performed (88-50460-88, eBioscience) as per the manufacturer's instructions. For quantification of cytokines in the tissue, mouse ears were flash-frozen in liquid nitrogen. Tissue was chopped, lysed, and homogenized in 500 ml of T-PER tissue protein extraction buffer (catalog no. 78510, Thermo Fisher Scientific) in the presence of complete protease inhibitor and phosphatase inhibitors. Total protein was quantified using a bicinchoninic acid protein assay kit (catalog no. 23227, Pierce), and levels of IL-5 were enumerated after normalizing to the total protein content in the tissue. IL-5 levels in ear skin were measured using Quantikine IL-5 kit (M5000, R&D Systems), and TL1A levels were measured using DuoSet ELISA kit (DY1896-05, R&D Systems).

Statistical analysis

Statistical significance was determined by the Mann-Whitney test or analysis of variance (ANOVA) analysis using GraphPad Prism. $P < 0.05$ was considered statistically significant.

Supplementary Material

Refer to Web version on PubMed Central for supplementary material.

Acknowledgments

We thank the flow cytometry core at Boston Children's Hospital, the sequencing core at Dana-Farber Cancer Institute, and the Human Skin Disease Resource Core at Brigham and Women's Hospital for their service; T. Chatila for a gift of *Foxp3*^{egfp} mice; D. O'Leary for a gift of *Rora*$^{Cre/Cre}$ mice; R. Clark for sharing human skin samples; and T. Chatila, L. M. Charbonnier, H. Oettgen, and J. Chou for reading the manuscript and useful discussions.

Funding: This work was supported by NIH grant AI113294-01A1, HHSN272201000020C, and intramural funding from the National Institute of Arthritis and Musculoskeletal and Skin Diseases, NIH.

REFERENCES AND NOTES

1. Spergel JM, Paller AS. Atopic dermatitis and the atopic march. J Allergy Clin Immunol. 2003; 112:S118–S127. [PubMed: 14657842]
2. Salimi M, Barlow JL, Saunders SP, Xue L, Gutowska-Owsiak D, Wang X, Huang LC, Johnson D, Scanlon ST, McKenzie ANJ, Fallon PG, Ogg GS. A role for IL-25 and IL-33–driven type-2 innate lymphoid cells in atopic dermatitis. J Exp Med. 2013; 210:2939–2950. [PubMed: 24323357]
3. Roediger B, Kyle R, Yip KH, Sumaria N, Guy TV, Kim BS, Mitchell AJ, Tay SS, Jain R, Forbes-Blom E, Chen X, Tong PL, Bolton HA, Artis D, Paul WE, Fazekas de St Groth B, Grimbaldeston MA, Le Gros G, Weninger W. Cutaneous immunosurveillance and regulation of inflammation by group 2 innate lymphoid cells. Nat Immunol. 2013; 14:564–573. [PubMed: 23603794]
4. Kim BS, Siracusa MC, Saenz SA, Noti M, Monticelli LA, Sonnenberg GF, Hepworth MR, Van Voorhees AS, Comeau MR, Artis D. TSLP elicits IL-33–independent innate lymphoid cell responses to promote skin inflammation. Sci Transl Med. 2013; 5:170ra16.

5. Li M, Hener P, Zhang Z, Kato S, Metzger D, Chambon P. Topical vitamin D3 and low-calcemic analogs induce thymic stromal lymphopoietin in mouse keratinocytes and trigger an atopic dermatitis. Proc Natl Acad Sci U.S.A. 2006; 103:11736–11741. [PubMed: 16880407]
6. Leyva-Castillo JM, Li M. Thymic stromal lymphopoietin and atopic diseases. Rev Fr Allergol. 2014; 54:364–376.
7. Bartnikas LM, Gurish MF, Burton OT, Leisten S, Janssen E, Oettgen HC, Beaupré J, Lewis CN, Austen KF, Schulte S, Hornick JL, Geha RS, Oyoshi MK. Epicutaneous sensitization results in IgE-dependent intestinal mast cell expansion and food-induced anaphylaxis. J Allergy Clin Immunol. 2013; 131:451–460.e6. [PubMed: 23374269]
8. Spergel JM, Mizoguchi E, Brewer JP, Martin TR, Bhan AK, Geha RS. Epicutaneous sensitization with protein antigen induces localized allergic dermatitis and hyperresponsiveness to methacholine after single exposure to aerosolized antigen in mice. J Clin Invest. 1998; 101:1614–1622. [PubMed: 9541491]
9. Leyva-Castillo JM, Hener P, Jiang H, Li M. TSLP produced by keratinocytes promotes allergen sensitization through skin and thereby triggers atopic march in mice. J Invest Dermatol. 2013; 133:154–163. [PubMed: 22832486]
10. Woodward AL, Spergel JM, Alenius H, Mizoguchi E, Bhan AK, Castigli E, Brodeur SR, Oettgen HC, Geha RS. An obligate role for T-cell receptor $\alpha\beta^+$ T cells but not T-cell receptor $\gamma\delta^+$ T cells, B cells, or CD40/CD40L interactions in a mouse model of atopic dermatitis. J Allergy Clin Immunol. 2001; 107:359–366. [PubMed: 11174205]
11. Panduro M, Benoist C, Mathis D. Tissue Tregs. Annu Rev Immunol. 2016; 34:609–633. [PubMed: 27168246]
12. Chatila TA, Blaeser F, Ho N, Lederman HM, Voulgaropoulos C, Helms C, Bowcock AM. *JM2*, encoding a fork head–related protein, is mutated in X-linked autoimmunity–allergic disregulation syndrome. J Clin Invest. 2000; 106:R75–R81. [PubMed: 11120765]
13. Godfrey VL, Wilkinson JE, Russell LB. X-linked lymphoreticular disease in the scurfy (sf) mutant mouse. Am J Pathol. 1991; 138:1379–1387. [PubMed: 2053595]
14. Szegedi A, Baráth S, Nagy G, Szodoray P, Gál M, Sipka S, Bagdi E, Banham AH, Krenács L. Regulatory T cells in atopic dermatitis: Epidermal dendritic cell clusters may contribute to their local expansion. Br J Dermatol. 2009; 160:984–993. [PubMed: 19222459]
15. Sanchez Rodriguez R, Pauli ML, Neuhaus IM, Yu SS, Arron ST, Harris HW, Yang SH-Y, Anthony BA, Sverdrup FM, Krow-Lucal E, MacKenzie TC, Johnson DS, Meyer EH, Löhr A, Hsu A, Koo J, Liao W, Gupta R, Debbaneh MG, Butler D, Huynh M, Levin EC, Leon A, Hoffman WY, McGrath MH, Alvarado MD, Ludwig CH, Truong H-A, Maurano MM, Gratz IK, Abbas AK, Rosenblum MD. Memory regulatory T cells reside in human skin. J Clin Invest. 2014; 124:1027–1036. [PubMed: 24509084]
16. Wong SH, Walker JA, Jolin HE, Drynan LF, Hams E, Camelo A, Barlow JL, Neill DR, Panova V, Koch U, Radtke F, Hardman CS, Hwang YY, Fallon PG, McKenzie ANJ. Transcription factor RORα is critical for nuocyte development. Nat Immunol. 2012; 13:229–236. [PubMed: 22267218]
17. Yang XO, Nurieva R, Martinez GJ, Kang HS, Chung Y, Pappu BP, Shah B, Chang SH, Schluns KS, Watowich SS, Feng XH, Jetten AM, Dong C. Molecular antagonism and plasticity of regulatory and inflammatory T cell programs. Immunity. 2008; 29:44–56. [PubMed: 18585065]
18. Dussault I, Fawcett D, Matthyssen A, Bader JA, Giguère V. Orphan nuclear receptor RORα-deficient mice display the cerebellar defects of. staggerer Mech Dev. 1998; 70:147–153. [PubMed: 9510031]
19. Rubtsov YP, Rasmussen JP, Chi EY, Fontenot J, Castelli L, Ye X, Treuting P, Siewe L, Roers A, Henderson WR Jr, Muller W, Rudensky AY. Regulatory T cell-derived interleukin-10 limits inflammation at environmental interfaces. Immunity. 2008; 28:546–558. [PubMed: 18387831]
20. Rothenberg ME, Luster AD, Leder P. Murine eotaxin: An eosinophil chemoattractant inducible in endothelial cells and in interleukin 4-induced tumor suppression. Proc Natl Acad Sci U.S.A. 1995; 92:8960–8964. [PubMed: 7568052]
21. Nussbaum JC, Van Dyken SJ, von Moltke J, Cheng LE, Mohapatra A, Molofsky AB, Thornton EE, Krummel MF, Chawla A, Liang HE, Locksley RM. Type 2 innate lymphoid cells control eosinophil homeostasis. Nature. 2013; 502:245–248. [PubMed: 24037376]

22. Mould AW, Matthaei KI, Young IG, Foster PS. Relationship between interleukin-5 and eotaxin in regulating blood and tissue eosinophilia in mice. J Clin Invest. 1997; 99:1064–1071. [PubMed: 9062365]
23. Van Dyken SJ, Nussbaum JC, Lee J, Molofsky AB, Liang HE, Pollack JL, Gate RE, Haliburton GE, Ye CJ, Marson A, Erle DJ, Locksley RM. A tissue checkpoint regulates type 2 immunity. Nat Immunol. 2016; 17:1381–1387. [PubMed: 27749840]
24. Islam SA, Chang DS, Colvin RA, Byrne MH, McCully ML, Moser B, Lira SA, Charo IF, Luster AD. Mouse CCL8, a CCR8 agonist, promotes atopic dermatitis by recruiting IL-5^{+} T_H2 cells. Nat Immunol. 2011; 12:167–177. [PubMed: 21217759]
25. Jetten AM. Retinoid-related orphan receptors (RORs): Critical roles in development, immunity, circadian rhythm, and cellular metabolism. Nucl Recept Signal. 2009; 7:e003. [PubMed: 19381306]
26. Huynh A, DuPage M, Priyadharshini B, Sage PT, Quiros J, Borges CM, Townamchai N, Gerriets VA, Rathmell JC, Sharpe AH, Bluestone JA, Turka LA. Control of PI(3) kinase in T_{reg} cells maintains homeostasis and lineage stability. Nat Immunol. 2015; 16:188–196. [PubMed: 25559257]
27. Scharschmidt TC, Vasquez KS, Pauli ML, Leitner EG, Chu K, Truong H-A, Lowe MM, Sanchez Rodriguez R, Ali N, Laszik ZG, Sonnenburg JL, Millar SE, Rosenblum MD. Commensal microbes and hair follicle morphogenesis coordinately drive Treg migration into neonatal skin. Cell Host Microbe. 2017; 21:467–477.e5. [PubMed: 28343820]
28. Deaglio S, Dwyer KM, Gao W, Friedman D, Usheva A, Erat A, Chen JF, Enjyoji K, Linden J, Oukka M, Kuchroo VK, Strom TB, Robson SC. Adenosine generation catalyzed by CD39 and CD73 expressed on regulatory T cells mediates immune suppression. J Exp Med. 2007; 204:1257–1265. [PubMed: 17502665]
29. Gavin MA, Rasmussen JP, Fontenot JD, Vasta V, Manganiello VC, Beavo JA, Rudensky AY. Foxp3-dependent programme of regulatory T-cell differentiation. Nature. 2007; 445:771–775. [PubMed: 17220874]
30. Noval Rivas M, Burton OT, Oettgen HC, Chatila T. IL-4 production by group 2 innate lymphoid cells promotes food allergy by blocking regulatory T-cell function. J Allergy Clin Immunol. 2016; 138:801–811.e9. [PubMed: 27177780]
31. Noval Rivas M, Burton OT, Wise P, Charbonnier L-M, Georgiev P, Oettgen HC, Rachid R, Chatila TA. Regulatory T cell reprogramming toward a Th2-cell-like lineage impairs oral tolerance and promotes food allergy. Immunity. 2015; 42:512–523. [PubMed: 25769611]
32. Kitoh A, Ono M, Naoe Y, Ohkura N, Yamaguchi T, Yaguchi H, Kitabayashi I, Tsukada T, Nomura T, Miyachi Y, Taniuchi I, Sakaguchi S. Indispensable role of the Runx1-Cbfβ transcription complex for in vivo-suppressive function of FoxP3^{+} regulatory T cells. Immunity. 2009; 31:609–620. [PubMed: 19800266]
33. Meylan F, Hawley ET, Barron L, Barlow JL, Penumetcha P, Pelletier M, Sciumè G, Richard AC, Hayes ET, Gomez-Rodriguez J, Chen X, Paul WE, Wynn TA, McKenzie ANJ, Siegel RM. The TNF-family cytokine TL1A promotes allergic immunopathology through group 2 innate lymphoid cells. Mucosal Immunol. 2014; 7:958–968. [PubMed: 24368564]
34. Schreiber TH, Wolf D, Tsai MS, Chirinos J, Deyev VV, Gonzalez L, Malek TR, Levy RB, Podack ER. Therapeutic Treg expansion in mice by TNFRSF25 prevents allergic lung inflammation. J Clin Invest. 2010; 120:3629–3640. [PubMed: 20890040]
35. Lim AI, Menegatti S, Bustamante J, Le Bourhis L, Allez M, Rogge L, Casanova JL, Yssel H, Di Santo JP. IL-12 drives functional plasticity of human group 2 innate lymphoid cells. J Exp Med. 2016; 213:569–583. [PubMed: 26976630]
36. Yu X, Pappu R, Ramirez-Carrozzi V, Ota N, Caplazi P, Zhang J, Yan D, Xu M, Lee WP, Grogan JL. TNF superfamily member TL1A elicits type 2 innate lymphoid cells at mucosal barriers. Mucosal Immunol. 2014; 7:730–740. [PubMed: 24220298]
37. Hirahara K, Liu L, Clark RA, Yamanaka K-i, Fuhlbrigge RC, Kupper TS. The majority of human peripheral blood CD4^{+}CD25^{high}Foxp3^{+} regulatory T cells bear functional skin-homing receptors. J Immunol. 2006; 177:4488–4494. [PubMed: 16982885]

38. Mochizuki M, Bartels J, Mallet AI, Christophers E, Schröder JM. IL-4 induces eotaxin: A possible mechanism of selective eosinophil recruitment in helminth infection and atopy. J Immunol. 1998; 160:60–68. [PubMed: 9551956]

39. Gandhi R, Kumar D, Burns EJ, Nadeau M, Dake B, Laroni A, Kozoriz D, Weiner HL, Quintana FJ. Activation of the aryl hydrocarbon receptor induces human type 1 regulatory T cell–like and Foxp3^{+} regulatory T cells. Nat Immunol. 2010; 11:846–853. [PubMed: 20676092]

40. Kolodin D, van Panhuys N, Li C, Magnuson AM, Cipolletta D, Miller CM, Wagers A, Germain RN, Benoist C, Mathis D. Antigen- and cytokine-driven accumulation of regulatory T cells in visceral adipose tissue of lean mice. Cell Metab. 2015; 21:543–557. [PubMed: 25863247]

41. Moffatt MF, Gut IG, Demenais F, Strachan DP, Bouzigon E, Heath S, von Mutius E, Farrall M, Lathrop M, Cookson WOCM, GABRIEL Consortium. A large-scale, consortium-based genomewide association study of asthma. N Engl J Med. 2010; 363:1211–1221. [PubMed: 20860503]

42. Majewska A, Gajewska M, Dembele K, Maciejewski H, Prostek A, Jank M. Lymphocytic, cytokine and transcriptomic profiles in peripheral blood of dogs with atopic dermatitis. BMC Vet Res. 2016; 12:174. [PubMed: 27553600]

43. Schiering C, Krausgruber T, Chomka A, Fröhlich A, Adelmann K, Wohlfert EA, Pott J, Griseri T, Bollrath J, Hegazy AN, Harrison OJ, Owens BMJ, Löhning M, Belkaid Y, Fallon PG, Powrie F. The alarmin IL-33 promotes regulatory T-cell function in the intestine. Nature. 2014; 513:564–568. [PubMed: 25043027]

44. Mukherji A, Kobiita A, Ye T, Chambon P. Homeostasis in intestinal epithelium is orchestrated by the circadian clock and microbiota cues transduced by TLRs. Cell. 2013; 153:812–827. [PubMed: 23663780]

45. Chou S-J, Babot Z, Leingärtner A, Studer M, Nakagawa Y, O'Leary DDM. Geniculocortical input drives genetic distinctions between primary and higher-order visual areas. Science. 2013; 340:1239–1242. [PubMed: 23744949]

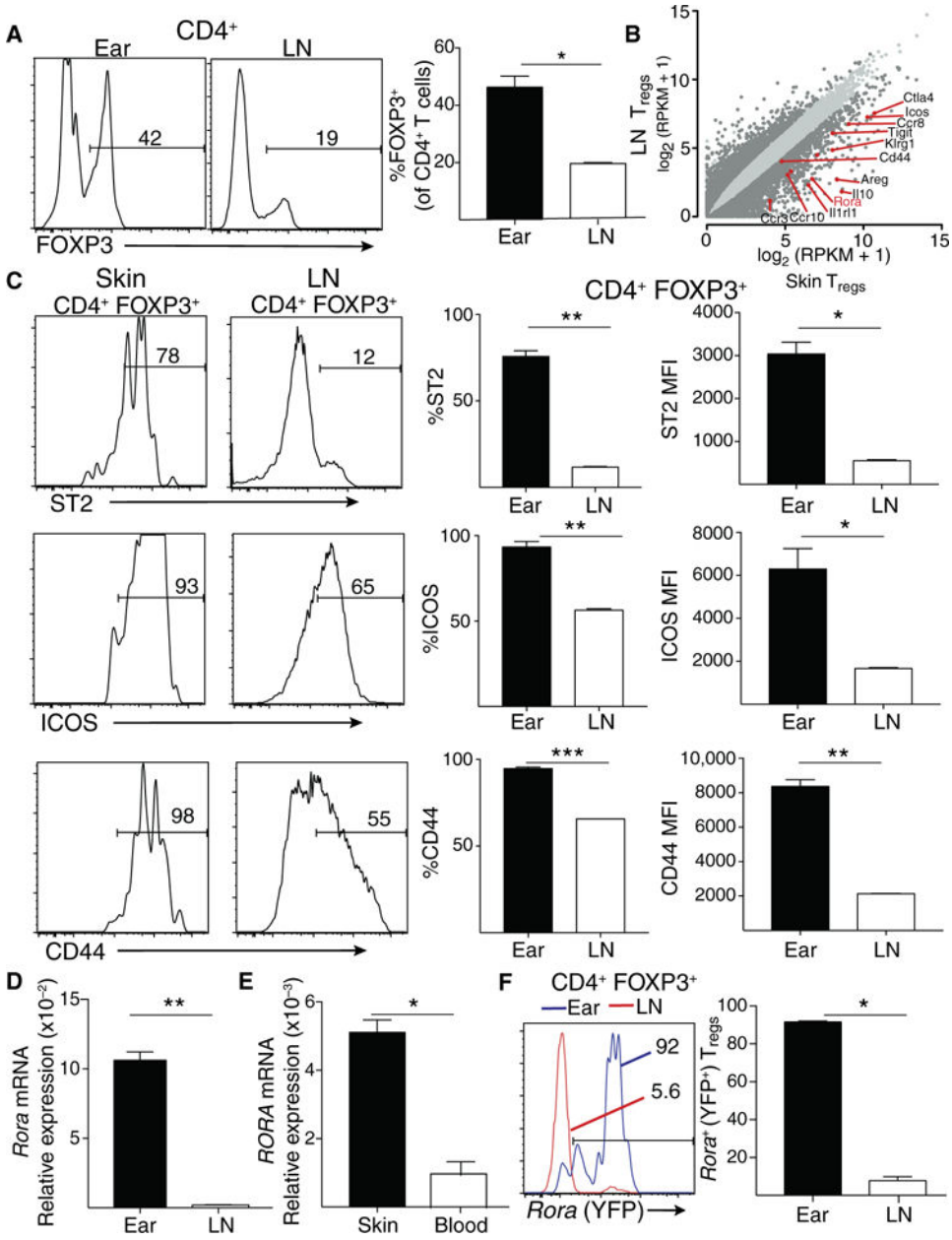

Fig. 1. Skin-resident T_{regs} exhibit an activated signature and express the transcription factor RORα

(**A**) Representative flow cytometric analysis (left) and quantification (right) of FOXP3$^+$ (CD3$^+$CD4$^+$YFP$^+$) cells among CD4$^+$ T cells in ear skin compared with dLNs from *Foxp3*$^{eyfp\text{-}cre}$ mice (n = 3 mice per group). (**B**) Scatterplot of $\log_2$ (RPKM + 1) values of genes expressed in skin T_{regs} (x axis) compared with LN T_{regs} (y axis) determined by NGS transcriptomic analysis. Genes that differ by more than twofold are shown in dark gray. Select genes are identified. (**C**) Representative flow cytometric analysis (left) and quantification (right) of CD44-, ICOS-, and ST2-expressing skin and dLNs T_{regs} and the mean fluorescence intensity (MFI) of these markers (n = 3 mice per group). (**D**) *Rora* expression levels in sorted T_{regs} from skin and dLNs from *Foxp3*$^{eyfp\text{-}cre}$ mice (n = 3 mice per

group). (**E**) *Rora* expression levels in sorted T_{regs} ($CD4^+CD25^+CD127^{lo}$) from blood and skin of healthy donors ($n = 2$). (**F**) Representative flow cytometric analysis (left) and quantification (right) of $Rora^+(YFP^+)$-expressing T_{regs} in skin and dLN of $Rora^{cre/cre}$ $Rosa^{yfp/yfp}$ mice ($n = 2$ mice per group). Columns and bars represent means and SEM. $^*P < 0.05$, $^{**}P < 0.01$, $^{***}P < 0.001$.

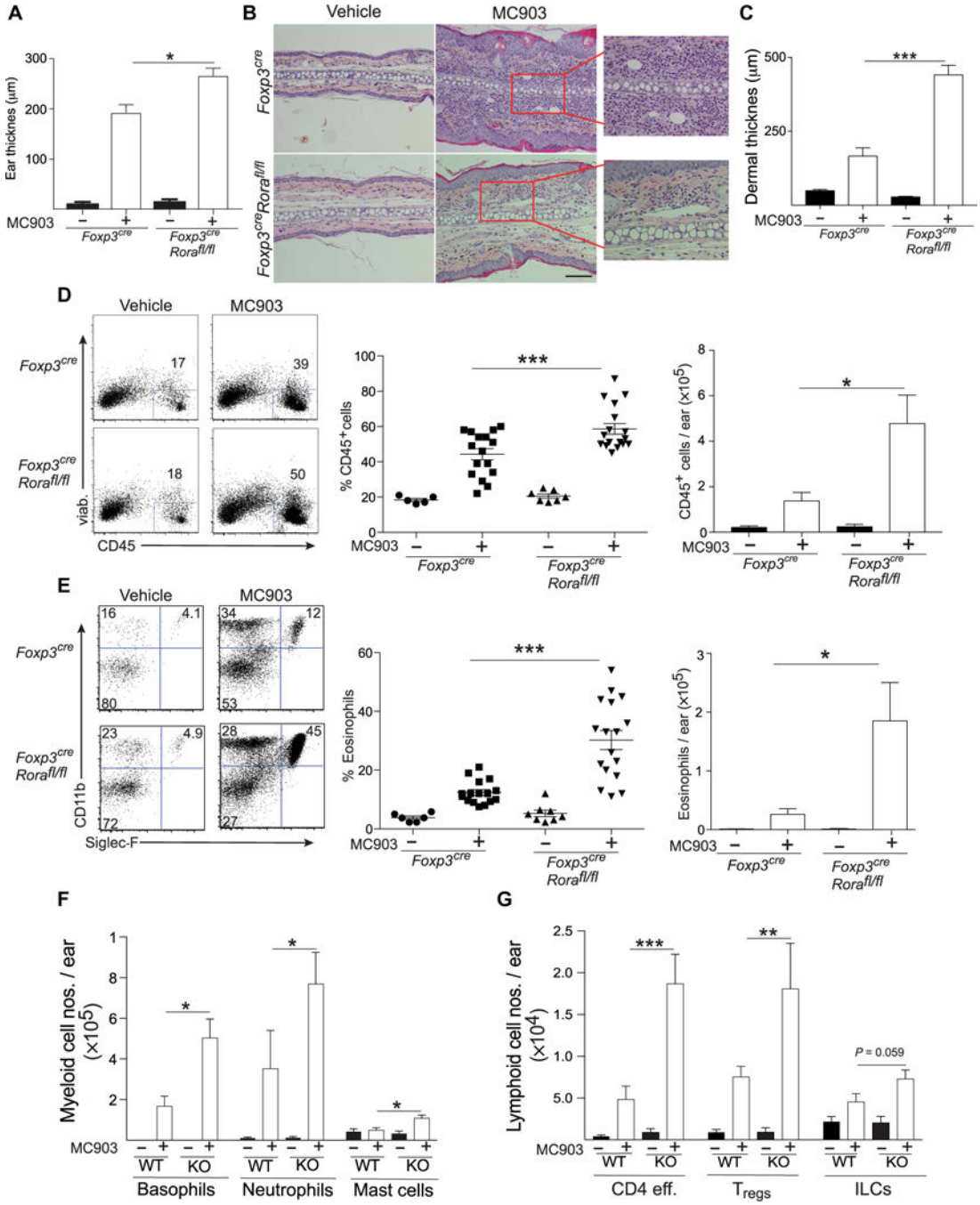

Fig. 2. RORα deficiency in T_{regs} results in exaggerated skin inflammation in response to topical application of MC903

(**A** to **G**) Quantification of ear thickness at day 7 (A); representative H&E-stained sections (B); quantification of dermal thickness (C); representative FACS analysis (left) and quantification of the percentages (middle) and numbers (right) of $CD45^+$ cells (D), eosinophils (E), mast cells, neutrophils, and basophils (F), and $CD4^+FOXP3^+$ T_{regs}, $CD4^+FOXP3^-$ T_{effs}, and ILCs (G) in vehicle or MC903-treated ears of *Foxp3*$^{eyfp\text{-}cre}$*Rora*$^{fl/fl}$

mice and *Foxp3*$^{eyfp\text{-}cre}$ controls. $n = 3$ to 8 mice per group. Columns and bars represent means and SEM. $^{*}P < 0.05$, $^{***}P < 0.001$.

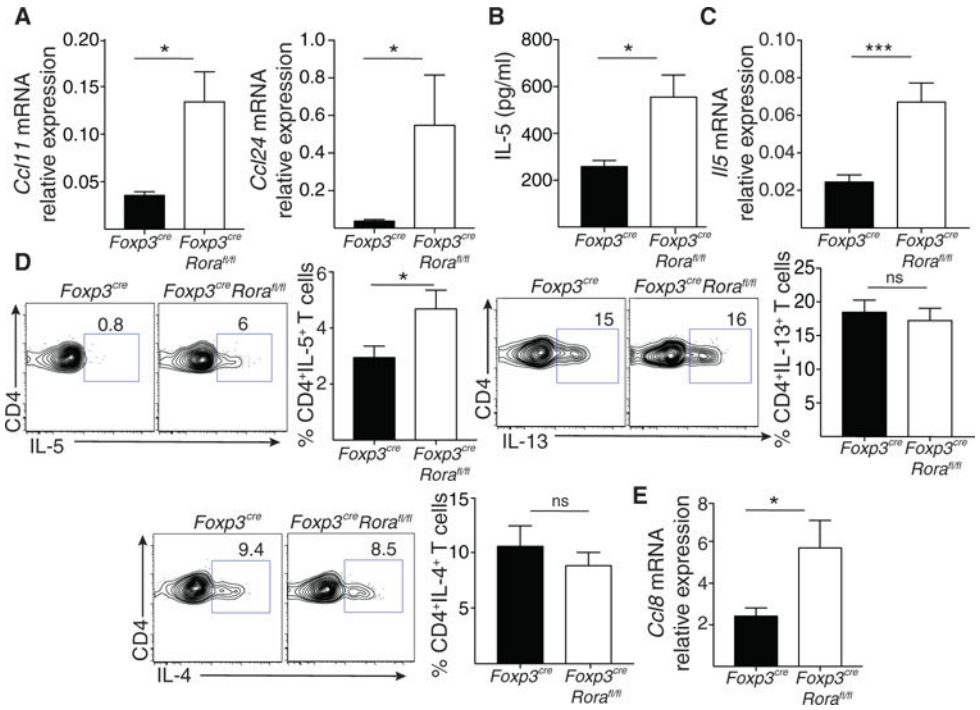

Fig. 3. Increased expression of eotaxins and IL-5 in MC903-treated skin of *Foxp3*$^{eyfp\text{-}cre}$*Rora*$^{fl/fl}$ mice. (**A** to **E**) Relative *Ccl11* and *Ccl24* mRNA expression (A); IL-5 levels (B); relative *Il5* expression in sorted Lin^{-}CD90^{+} ILCs (C); representative FACS analysis and quantitation of the percentages of CD4^{+}IL-5^{+}, CD4^{+}IL-13^{+}, and CD4^{+}IL-4^{+} T_{effs} (D); and relative *Ccl8* mRNA expression in MC903- treated skin of *Foxp3*$^{eyfp\text{-}cre}$*Rora*$^{fl/fl}$ mice and *Foxp3*$^{eyfp\text{-}cre}$ controls (E). $n = 4$ to 7 mice per group. Columns and bars represent means and SEM. $^{*}P < 0.05$, $^{***}P < 0.001$. ns, not significant.

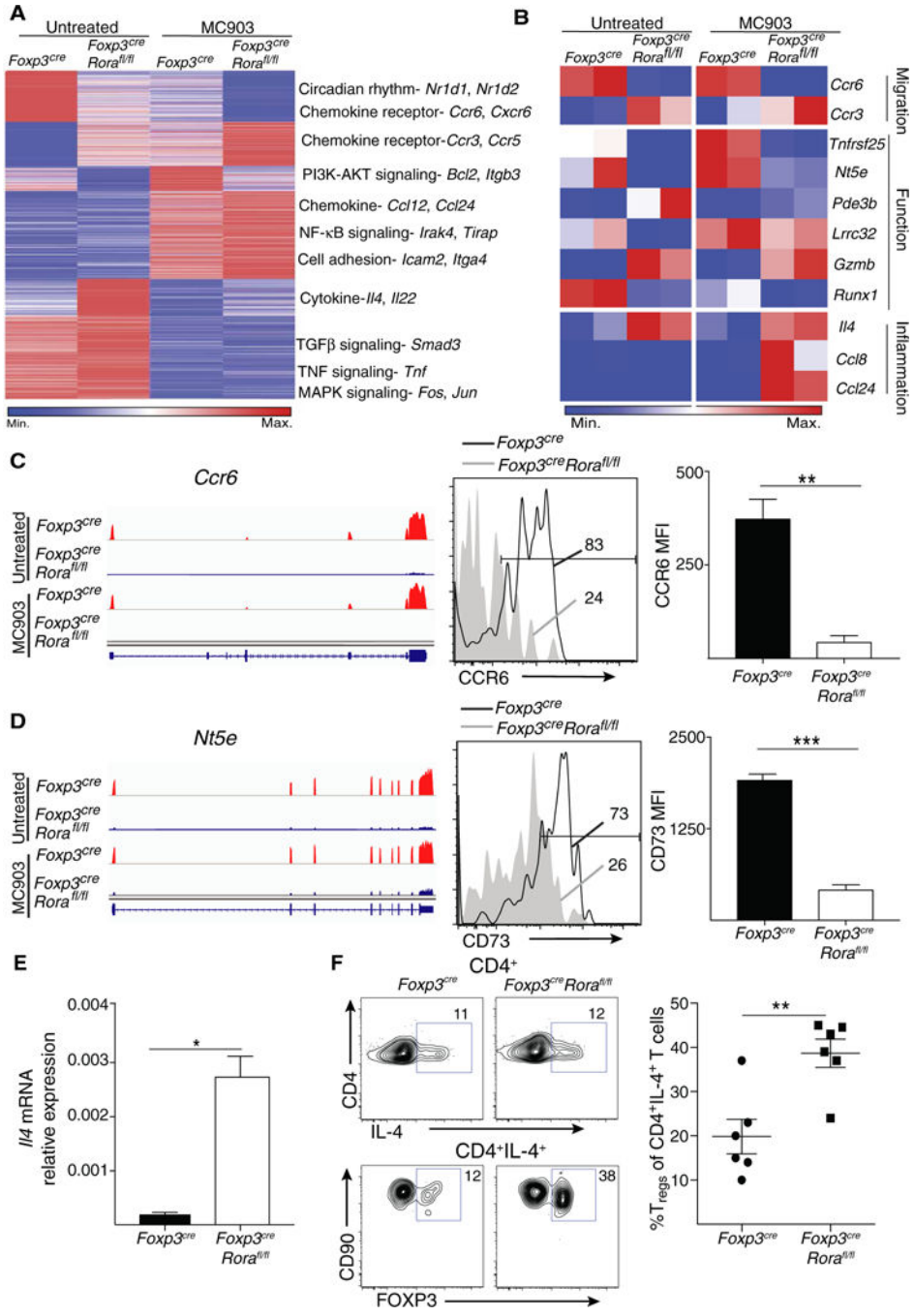

Fig. 4. RORα deficiency in T_{regs} alters the expression of genes involved in T_{reg} cell migration and function and skews T_{regs} to IL-4–producing effectors

(**A**) Heat map showing relative expression of genes clustered by *K*-mean values in skin T_{regs} of *Foxp3*$^{eyfp\text{-}cre}$ and *Foxp3*$^{eyfp\text{-}cre}$*Rora*$^{fl/fl}$ mice in the steady state and after MC903 treatment (*n* = 4 to 5 mice per group). (**B**) Heat map showing the relative expression of select chemotaxis, function, and inflammation genes in skin T_{regs} from *Foxp3*$^{eyfp\text{-}cre}$*Rora*$^{fl/fl}$ mice and controls (*n* = 4 to 5 mice per group). (**C** and **D**) RNA-seq tracing of *Ccr6* and *Nt5e* expression (left), representative FACS analysis (middle), and MFIs (right) of CCR6 and

CD73 expression in skin T_{regs} of *Foxp3*$^{eyfp\text{-}cre}$ and *Foxp3*$^{eyfp\text{-}cre}$*Rora*$^{fl/fl}$ mice (n = 4 to 5 mice per group). The numbers in the FACS panels represent the percentage of positive cells relative to fluorescence minus one (FMO) control. (**E**) Relative *Il4* mRNA levels in T_{regs} from MC903-treated skin of *Foxp3*$^{eyfp\text{-}cre}$*Rora*$^{fl/fl}$ mice and controls (n = 4 to 5 mice per group). (**F**) Representative FACS analysis of IL-4 expression in $CD4^+$ cells and of FOXP3 versus CD90 expression in IL-4^+CD4^+ cells (left) and quantitation of the percentage of IL-$4^+CD4^+FOXP3^+$ cells among IL-4^+CD4^+ cells in the skin of MC903-treated *Foxp3*$^{eyfp\text{-}cre}$*Rora*$^{fl/fl}$ mice and controls.

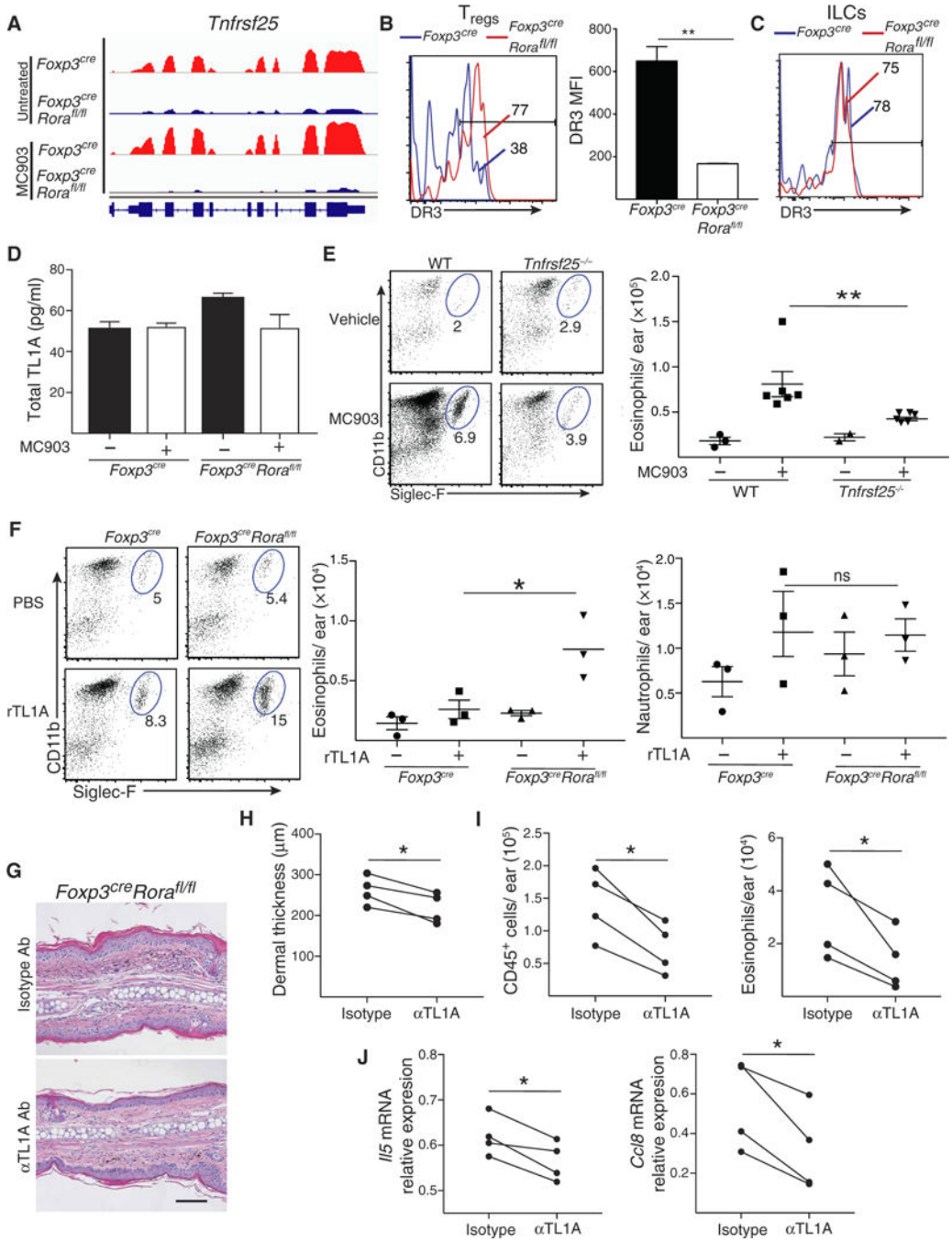

Fig. 5. RORα expression in T_{regs} promotes expression of the TL1A receptor DR3 and restrains TL1A-driven allergic inflammation elicited by cutaneous application of MC903

(**A**) RNA-seq tracing of *Tnfrsf25* expression in skin T_{regs} from untreated and MC903-treated skin of *Foxp3*$^{eyfp\text{-}cre}$ and *Foxp3*$^{eyfp\text{-}cre}$*Rora*$^{fl/fl}$ mice. (**B**) Representative FACS analysis (left) and MFIs (right) of DR3 expression by skin T_{regs} of *Foxp3*$^{eyfp\text{-}cre}$*Rora*$^{fl/fl}$ mice and *Foxp3*$^{eyfp\text{-}cre}$ controls (n = 3 mice per group). The numbers in the FACS panels represent the percentage of positive cells relative to FMO control. (**C**) Representative FACS analysis of DR3 expression by ILCs from the skin of *Foxp3*$^{eyfp\text{-}cre}$*Rora*$^{fl/fl}$ mice and *Foxp3*$^{eyfp\text{-}cre}$

controls. Results are representative of three independent experiments. The numbers in the FACS panels represent the percentage of positive cells relative to FMO control. (**D**) TL1A levels in vehicle and MC903-treated ear skin of *Foxp3*$^{eyfp\text{-}cre}$*Rora*$^{fl/fl}$ mice and *Foxp3*$^{eyfp\text{-}cre}$ controls (n = 4 mice per group). (**E**) Representative FACS analysis (left) and quantification (right) of CD11b^{+}Siglec-F^{+} eosinophils in MC903-treated ears of *Tnfrsf25*$^{-/-}$ mice and WT controls. (**F**) Representative FACS analysis (left) and quantification (right) of CD11b^{+}Siglec-F^{+} eosinophils and CD11b^{+}Gr1^{high} neutrophils in TL1A-injected skin of *Foxp3*$^{eyfp\text{-}cre}$*Rora*$^{fl/fl}$ mice and *Foxp3*$^{eyfp\text{-}cre}$ controls (n = 3 mice per group). (**G** to **J**) Representative H&E-stained sections (G), quantification of dermal thickness (H), quantification of CD45^{+} cells (right) and CD11b^{+}Siglec-F^{+} eosinophils (left) (I), and relative mRNA expression of *Il5* (right) and *Ccl8* (left) (J) in MC903- treated ears of *Foxp3*$^{eyfp\text{-}cre}$*Rora*$^{fl/fl}$ mice injected with anti-TL1A antibody or isotype control (n = 4 mice per group). Columns and bars represent means and SEM. $^{*}P < 0.05$, $^{**}P < 0.01$

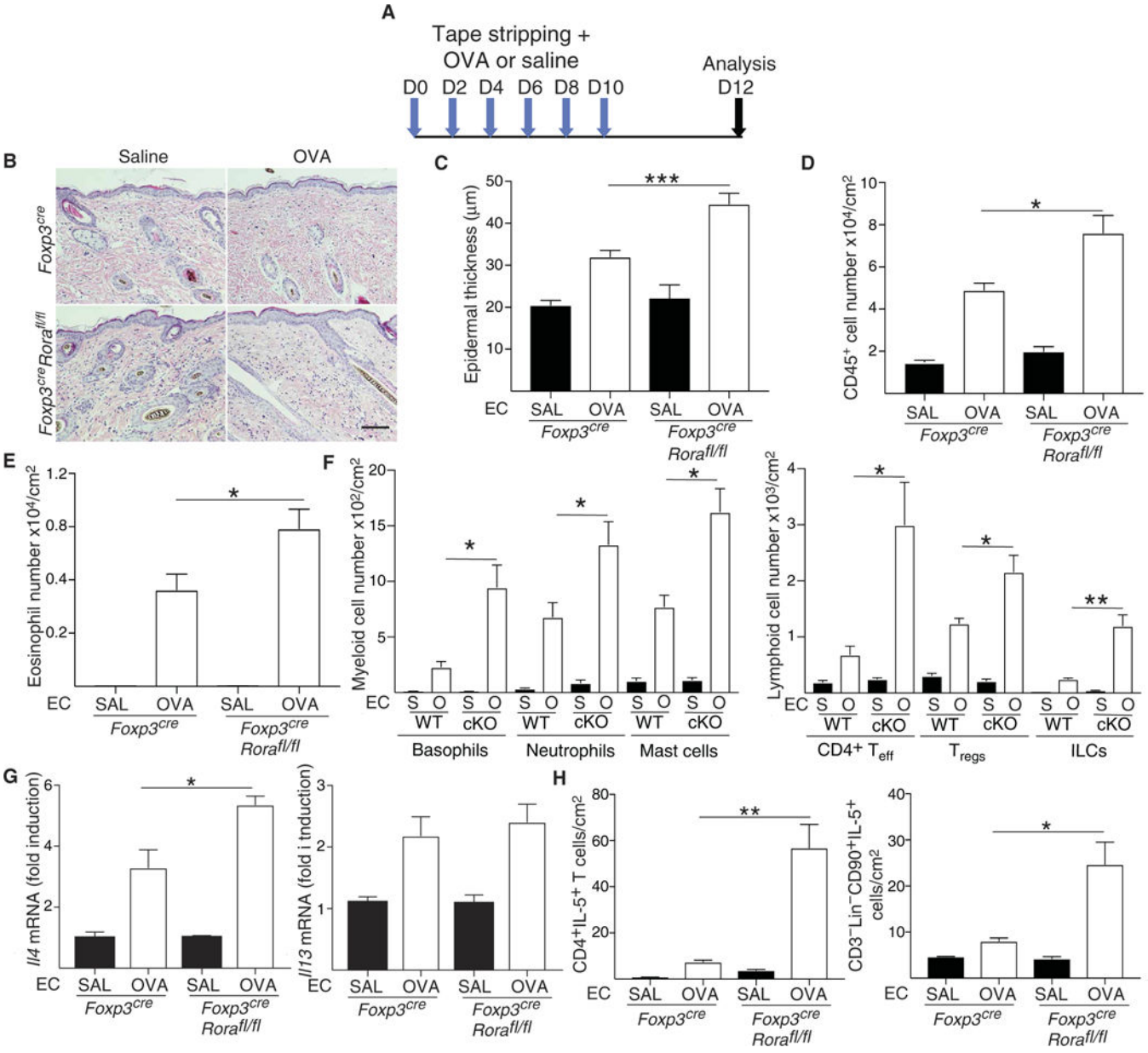

Fig. 6. RORα deficiency in T_{regs} results in exaggerated skin inflammation in response to EC sensitization

(**A**) Schematic of the experimental mouse model. (**B** to **H**) Representative H&E-stained sections (B); quantification of epidermal thickness (C); number of $CD45^+$ cells (D), $CD11b^+Siglec\text{-}F^+$ eosinophils (E), mast cells, neutrophils, and basophils (left), and $CD4^+FOXP3^-$ T_{effs}, $CD4^+FOXP3^+$ T_{regs}, and ILCs (right) (F); relative *Il4* (right) and *Il13* (left) mRNA expression (G); and numbers of IL-5^+ $CD4^+$ T cells and ILCs (H) in saline and OVA-sensitized skin of *Foxp3*$^{eyfp\text{-}cre}$*Rora*$^{fl/fl}$ mice (also designated as cKO) and *Foxp3*$^{eyfp\text{-}cre}$ controls (also designated as WT). $n = 3$ to 7 mice per group. Columns and bars represent means and SEM. $^*P < 0.05$, $^{***}P < 0.001$.